

OPTICAL AND STRUCTURAL PROPERTIES OF Er³⁺-DOPED GaN GROWN BY MBE

R. H. Birkhahn, R. Hudgins, D. S. Lee, B.K. Lee and A. J. Steckl*
A. Saleh**, R. G. Wilson**, J. M. Zavada***

*University of Cincinnati, Nanoelectronics Lab, Cincinnati, OH 45221-0030

**Charles Evans & Associates, Sunnyvale, CA 94086

***USARO, Research Triangle Park, NC 27709

Cite this article as: MRS Internet J. Nitride Semicond. Res. 4S1, G3.80(1999)

ABSTRACT

We report the morphological and compositional characteristics of Er-doped GaN grown by MBE on Si(111) substrates and their effect on optical properties. The GaN was grown by molecular beam epitaxy using solid sources (for Ga and Er) and a plasma gas source for N₂. The films emit by photoexcitation in the visible and near infrared wavelengths from the Er atomic levels. The morphology of the GaN:Er films was examined by AFM. Composition was determined by SIMS depth profiling that revealed a large Er concentration at 4.5×10^{21} atoms/cm³ accompanied by a high oxygen impurity concentration.

INTRODUCTION

Interest in GaN for optoelectronic devices has taken center stage recently since the fabrication of blue lasers by several research groups. These and other optical nitride devices are based on varying Al, In, and Ga composition in heterostructures to achieve wavelength-specific emission. Rare earth (RE) elements are also known to sharply emit light at specific wavelengths independent of the host, which is due to atomic transitions. As a result, devices based on RE materials should be easier to fabricate and require less materials or device design manipulation.

Rare earth elements have found wide use in a variety of light-emitting applications, from RE-doped fibers for infrared transmission to upconversion lasers to the phosphors found in CRT tubes. In most cases, the RE emits light at wavelengths specific to the atomic transitions between its 4f energy levels. For years, study of REs incorporated into a semiconductor matrix proceeded because of the possibility that carrier injection from the host could provide the energy necessary to stimulate emission. In addition, semiconductors can be easily integrated into existing electronics. Er is a rare earth well known¹ for its near-infrared (IR) emission (1.5 μm) which corresponds to the optical fiber loss minimum. Although other Er atomic levels exist, transitions with photonic emission from these states are normally observed only in glass hosts. Typically, the IR transitions seen from RE elements represent the lowest energy transition possible between 4f levels. Er incorporated into Si^{2,3,4,5} or GaAs^{6,7,8,9} has been the most commonly studied system, with its characteristic emission only well documented at infrared wavelengths.

Recently, we have reported^{10,11,12,13} the successful in-situ incorporation of Er into GaN by molecular beam epitaxy (MBE) on both sapphire and silicon, which produces room temperature visible and IR emission by both photoluminescence (PL) and electroluminescence (EL). We also have reported¹⁴ on Pr-doped GaN grown on Si (111) substrates and the resulting novel visible red emission at 650 nm by EL and PL, not previously observed outside of glass hosts.

Spectroscopically, these specific RE atomic levels in the visible region for Pr^{3+} ($^3\text{P}_0$) and Er^{3+} ($^2\text{H}_{11/2}$, $^4\text{S}_{3/2}$) are both known to have high likelihood of transition¹⁵ but, for reasons not yet clear, they are not observed when doped into other semiconductor hosts. The only previously reported system^{16,17,18,19} in which RE-doped semiconductors emit in the visible is ZnSe:Er.

EXPERIMENTAL

We have grown in situ-doped GaN:Er on a variety of substrates (Al_2O_3 , Si, 6H-SiC, HVPE GaN) by solid source and RF-assisted molecular beam epitaxy (MBE). The Riber MBE32 system used for growth has been described previously^{10,11}. The samples were pretreated by cleaning in acetone, methanol and deionized water before insertion into the loadlock. They were subsequently outgassed at $\sim 950^\circ\text{C}$ before growth. During growth, the Ga cell temperature was kept constant for a beam equivalent pressure of $\sim 8.2 \times 10^{-7}$ Torr. The rf-plasma source was kept constant at 400W with a N_2 flow rate of 1.5 sccm, corresponding to a chamber pressure of mid- 10^{-5} Torr. The growth temperature was varied from 750-950°C and the Er cell temperature was maintained at 1100°C.

For this paper, we have studied and characterized the GaN:Er films grown on Si (111) for their optical and compositional properties. The optical properties were characterized by photoluminescence (from UV to IR) at room temperature using a HeCd laser (325 nm). Structural properties were examined based on morphology and composition. Standard surface techniques were utilized for morphology and composition was determined by secondary ion mass spectrometry (SIMS).

RESULTS AND DISCUSSION

Optical

All the samples emit, regardless of substrate, at visible (green) and IR wavelengths corresponding to Er inner shell transitions. The green emission shown in Fig. 1 at 537 and 558 nm from the $^2\text{H}_{11/2}$ and the $^4\text{S}_{3/2}$ levels, respectively, is quite intense at room temperature. In addition to the Er^{3+} spectral lines, the scans also contained traces of GaN band edge emission near 370 nm and a broad background peaking near ~ 460 nm. The general trend of the visible and IR emission lines vs. substrate growth temperature is shown in Fig. 2. The visible 537 and 558 nm lines increase with growth temperature up to a certain cutoff after which emission is quenched. The open symbols represent one growth experiment in which the buffer layer was altered in an attempt to optimize conditions. Generally, the IR and the $^4\text{S}_{3/2}$ lines have opposite trends. This could be explained by visualizing¹⁰ the Er^{3+} energy level diagram. Carriers transferred from the GaN to the Er atoms cascade non-radiatively until they reach the $^2\text{H}_{11/2}$ and

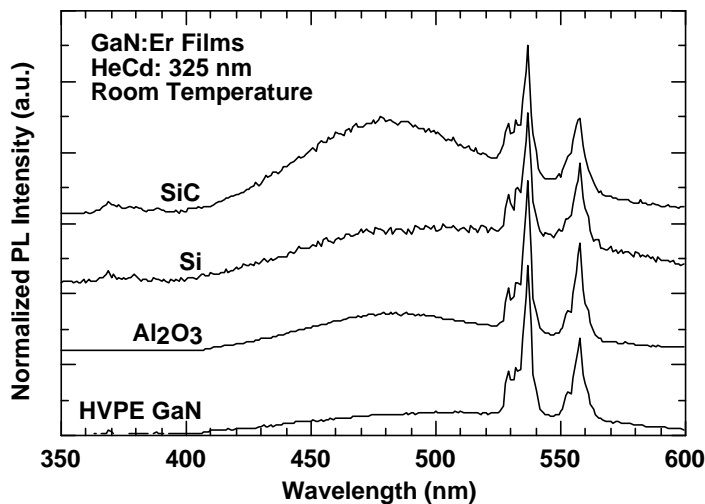


Figure 1: Visible PL spectrum of Er-doped GaN films. The PL is performed at room temperature with the He-Cd laser line at 325 nm.

$^4S_{3/2}$ states. At this point, two competitive processes occur: (a) de-excitation directly to the $^4I_{15/2}$ ground state or (b) cascading to the lowest excited state ($^4I_{13/2}$) followed by a radiative (at $1.54\ \mu\text{m}$) drop to the ground state. Carriers that radiate from the higher energy states decrease the number available for the $^4I_{13/2}$ state. This trend can also be seen in the buffer layer comparison at 750°C growth temperature: the increase in visible line intensity is accompanied by a decrease in IR emission.

Surface

Surface images of the GaN films were taken by scanning electron microscopy (SEM) and atomic force

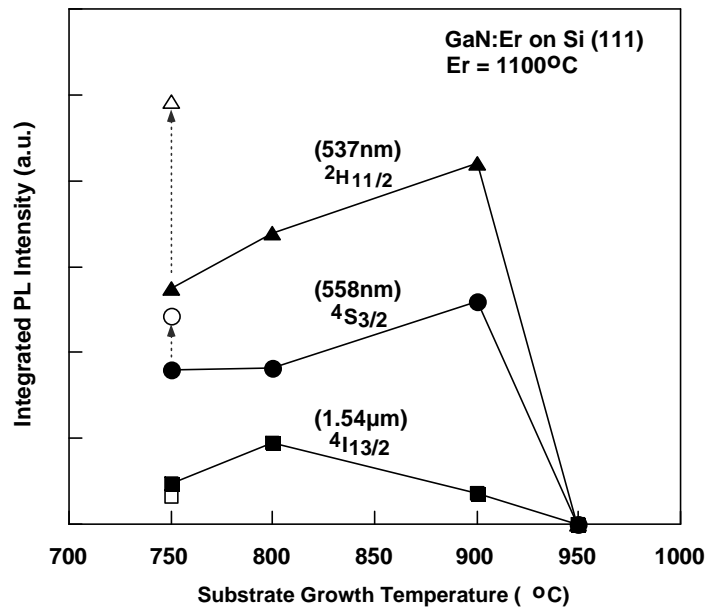


Figure 2: Integrated PL intensity of Er emission from samples grown on Si as a function of growth temperature. The open symbols represent a different buffer layer.

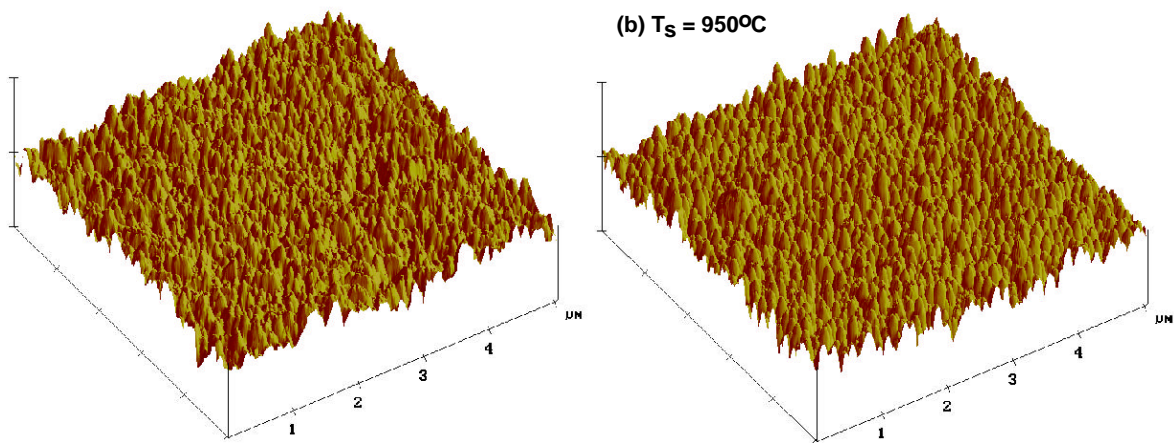


Figure 3: AFM images of the GaN:Er films on Si (111). Growth temperature was (a) 750°C and (b) 950°C . Er cell temperature was 1100°C .

microscopy (AFM). The SEM images were reported previously¹¹. AFM surface images of two GaN:Er films grown at 750°C and 950°C are shown in Fig. 3. The average roughness (R_a) of film surfaces for GaN grown at various temperatures is shown in Fig. 4. All scans were taken at random points from the center of the 2-inch wafers. The overall trend indicates that a growth temperature of 900°C leads to a maximum in surface roughness. GaN:Er films grown at 800°C or 1050°C exhibit an R_a one order of magnitude lower. Roughness appears to vary linearly with the Er concentration measured in GaN by SIMS (see Fig. 7). This corresponds well with our findings on sapphire²⁰.

Composition

A representative SIMS depth profile of the Er concentration of a GaN:Er film on Si is shown in Fig. 5. At this substrate temperature of 750°C, the Er incorporation profile is very uniform at a concentration of $\sim 6 \times 10^{20}$ atoms/cm³, corresponding to ~ 0.7 at.% throughout the film. For this set of experiments, the maximum Er concentration achieved was 5 at.% at a growth temperature of 900°C. The unintentional impurity concentrations of Si and O are shown in Fig. 6. The amount of Si observed in the GaN film is typically at the background limit of the measurement. However, there is evidence that the Si is diffusing into the GaN from the substrate. The maximum such diffusion measured is 1.2 μm into the film. The level of oxygen incorporated into the film is relatively high. The profile is also not uniform, which indicates a buildup of oxygen in the chamber during growth. The concentration

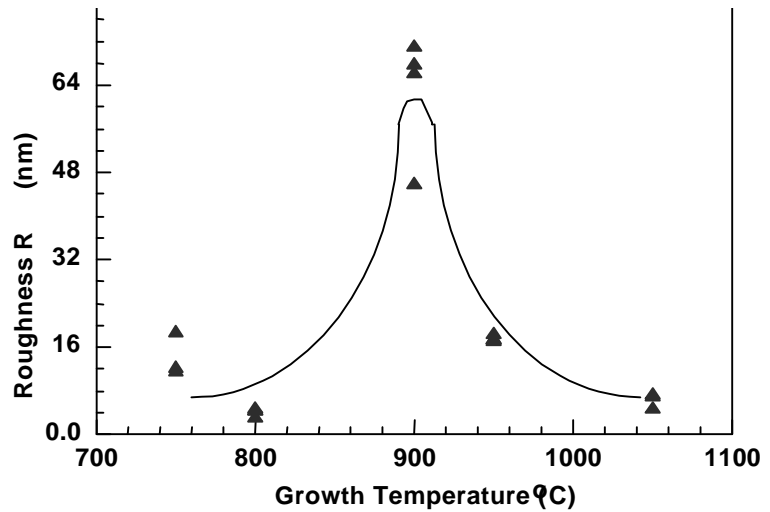


Figure 4: Average roughness (R_a) vs. substrate growth temperature by AFM of GaN:Er films on Si (111).

of oxygen tracks the amount of Er as seen in Fig. 7. At higher growth temperatures ($>900^\circ\text{C}$), the amount of Er drops even though the cell temperature remained constant at 1100°C. This indicates that oxygen can incorporate more readily at higher temperatures and that some thermal or surface kinetic process freezes out Er atoms. The solid source Er material is 99.9% pure and does contain trace amounts of oxygen and other impurities. This requires further investigation since oxygen has a known role in enhanced IR emission^{21,22,23,24} from Er in other

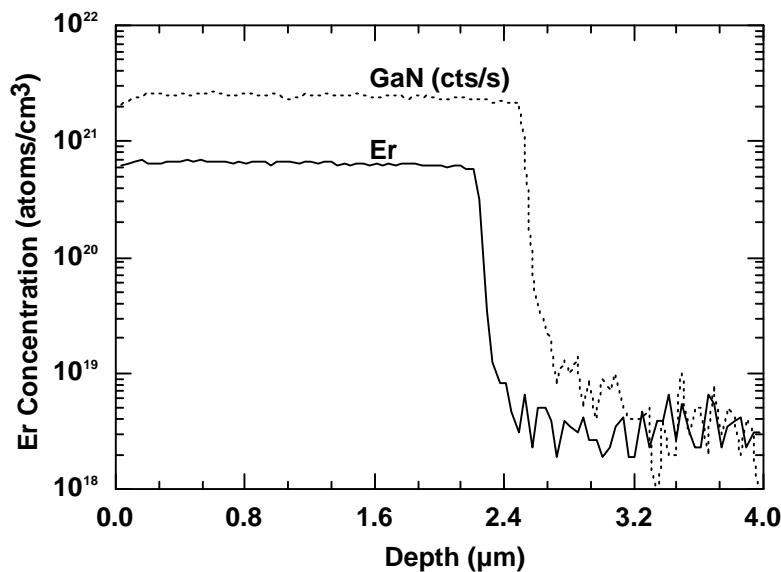


Figure 5: SIMS depth profile of Er concentration from film grown on Si. Er cell = 1100°C.

semiconductors.

SUMMARY

In summary, we have reported the optical, morphological, and compositional characteristics of Er-doped GaN grown by MBE on Si (111) substrates. We observed novel green emission from Er in GaN and demonstrated that the occurrence of this effect is independent of the substrate. Corresponding structural properties of the films on Si were examined by AFM. Composition data provided by SIMS demonstrated that we have incorporated a high concentration (5 at.%) of Er in GaN and revealed a relatively high level of

unintentional oxygen doping. Since emission from these films is already visible under ambient light, we expect that the intensity can be further optimized by choice of substrate, growth temperature, and Er flux.

This work was supported by a BMDO/ARO contract (L. Lome and J. Zavada) and a ARO AASERT grant. Equipment support was provided by an ARO URI grant and the Ohio Materials Network.

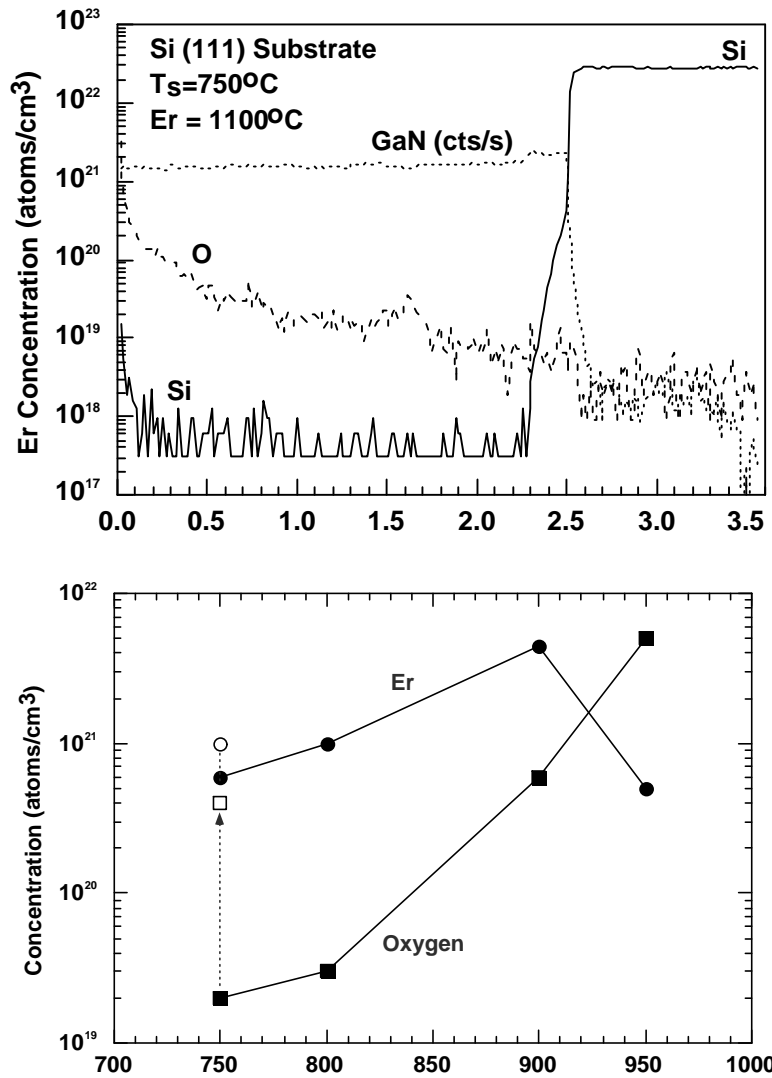


Figure 7: Concentration of Er and O as a function of growth temperature. The open symbols represent a different buffer layer. Er cell = 1100°C.

REFERENCES

- ¹ S. Coffa, G. Franzo, and F. Priolo, *MRS Bulletin* **23**, 25 (April 1998).
- ² F.Y.G. Ren, J. Michel, Q. Sun-Paduano, B. Zheng, H. Kitagawa, D.C. Jacobson, J.M. Poate and L.C. Kimerling, *Mat. Res. Soc. Symp. Proc.* **301**, 87 (1993).
- ³ G. Franzo, F. Priolo, S. Coffa, A. Polman and A. Carnera, *Appl. Phys. Lett.* **64** (17), 2235 (1994).
- ⁴ F. Priolo, G. Franzo, S. Coffa, A. Polman, V. Bellani, A. Carnera and C Spinella, *Mat. Res. Soc. Symp. Proc.* **316**, 397 (1994).
- ⁵ I.A. Buyanova, W.M. Chen, G. Pozina, W.X. Ni, G.V. Hansson and B. Monemar, *J. Vac. Sci. Tech. B* **16** (3), 1732 (1998).
- ⁶ R.S. Smith, H.D. Muller, H. Ennen, P. Wennekers and M. Maler, *Appl. Phys. Lett.* **50** (1), 49 (1987).
- ⁷ S.J. Chang and K. Takahei, *Appl. Phys. Lett.* **65** (4), 433 (1994).
- ⁸ D.W. Elsaesser, Y.K. Yeo, R.L. Hengehold, K.R. Evans and F.L. Pedrotti, *J. of Appl. Phys.* **77** (8), 3919 (1995).
- ⁹ K. Takahei and A. Taguchi, *J. of App. Phys.* **77** (4), 1735 (1995).
- ¹⁰ A.J. Steckl and R. Birkhahn, *Appl. Phys. Lett.* **73** (12), 1700 (1998).
- ¹¹ R. Birkhahn and A.J. Steckl, *Appl. Phys. Lett.* **73** (15), 2143 (1998).
- ¹² A. J. Steckl, M. Garter, R. Birkhahn and J. Scofield, *Appl. Phys. Lett.* **73** (17), 2450 (1998).
- ¹³ M. Garter, J. Scofield, R. Birkhahn and A. J. Steckl, *Appl. Phys. Lett.* **74** (2), (1999).
- ¹⁴ R. Birkhahn, M. Garter and A. J. Steckl. *Appl. Phys. Lett.* to be published.
- ¹⁵ K. A. Gschneidner and L. Eyring, **Vol. 11-Two-Hundred-Year Impact of Rare Earths on Science**, in *Handbook on the Physics and Chemistry of Rare Earths* North Holland Physics Publishing, New York, 1988.
- ¹⁶ J.D. Kingsley and M. Aven, *Phys. Rev.* **155** (2), 235 (1967).
- ¹⁷ M.R. Brown, A.F.J. Cox, W.A. Shand and J.M. Williams, *J. Physics C: Solid State Physics* **4**, 1049 (1971).
- ¹⁸ H. Kobayashi, S. Tanaka and H. Sasakura, *Jpn. J. Appl. Phys.* **12** (10), 1637 (1973).
- ¹⁹ I. Szczurek, H.J. Lozykowski and T. Szczurek, *J. Luminescence* **23**, 315 (1981).
- ²⁰ R. Birkhahn, R. Hudgins, D. Lee, A. J. Steckl, R. J. Molnar and J. M. Zavada, *J. Vac. Sci. and Tech. B*, to be published.
- ²¹ J. E. Colon, D. W. Elsaesser, Y. K. Yeo, R. L. Hengehold and G. S. Pomrenke, *Appl. Phys. Lett.* **62** (2), 216 (1993).
- ²² P. N. Favennec, H. L'Haridon, D. Moutonnet, M. Salvi and M. Gauneau, *Jpn. J. Appl. Phys.* **29** (4), L524 (1990).
- ²³ P.N. Favennec, H. L'Haridon, D. Moutonnet, M. Salvi and M. Gauneau, *Mat. Res. Soc. Symp. Proc.* **301**, 181 (1993).
- ²⁴ J. Michel, J. L. Benton, R. F. Ferrante, D. C. Jacobson, D. J. Eaglesham, E. A. Fitzgerald, Y. H. Xie, J. M. Poate and L. C. Kimerling, *J. Appl. Phys.* **70** (5), 2672 (1991).